Neoplasma 2024; 71(4): 333–346

doi:10.4149/neo_2024_230909N479

# Fluspirilene exerts an anti-glioblastoma effect through suppression of the FOXM1-KIF20A axis

Yang KONG[1,2], Wei ZHU[2], Zhen ZHANG[2,3], Wei SUN[2], Guangqiang CUI[2], Hongguang CHEN[2], Haiying WANG[4,*]

[1]*Intensive Care Unit-Laishan, The Affiliated Yantai Yuhuangding Hospital of Qingdao University, Yantai, China;* [2]*Department of Neurosurgery, The Affiliated Yantai Yuhuangding Hospital of Qingdao University, Yantai, China;* [3]*Pathology Department, The Affiliated Yantai Yuhuangding Hospital of Qingdao University, Yantai, China; 4Department of Anesthesiology, The Affiliated Yantai Yuhuangding Hospital of Qingdao University, Yantai, China.*

**Correspondence: 418273519@qq.com*

**Received September 9, 2023 / Accepted July 4, 2024**

Given the infiltrative nature of human glioblastoma (GBM), cocktail drug therapy will remain a vital tool for the treatment of the disease. We investigated fluspirilene, perphenazine, and sulpiride, three classic anti-schizophrenic drugs, as possible anti-GBM agents. The CCK-8 assay demonstrated that fluspirilene possesses the most outstanding anti-GBM effect. We performed molecular mechanisms studies *in vitro* and an orthotopic xenograft model in mice. Fluspirilene inhibited proliferation and migration *in vitro* in U87MG and U251 GBM cell lines. Flow cytometry demonstrated that treatment increased apoptosis and cells accumulated in the G2/M phase. Our analysis of publicly available expression data for several cell lines treated with the drug led to the identification of several genes, including *KIF20A*, that are downregulated by fluspirilene and lead to growth inhibition/apoptosis. We also demonstrated that siRNA knockdown of *KIF20A*, a member of the kinesin family, attenuated cell proliferation in GBM cells and an orthotopic xenograft model in mice. A regulator of *KIF20A*, the oncogenic transcription factor FOXM1, was identified using the String database, which harbors protein interaction networks. In fluspirilene-treated cells, FOXM1 protein was decreased, indicating that KIF20A was downregulated in the presence of the drug due to decreased FOXM1 protein. These results demonstrate that fluspirilene is an effective anti-GBM agent that works by suppressing the FOXM1-KIF20A oncogenic axis.

*Key words: glioblastoma; drug repurposing; antipsychotic drug; fluspirilene*

Glioblastoma (GBM) is the most aggressive malignant brain tumor in adults. With the general increase in the age of the human population, the incidence of the disease is on the rise. Despite multi-modality treatments including surgery, chemotherapy, and radiotherapy, the prognosis for GBM remains poor. The majority of patients diagnosed with GBM die within 2 years [1]. Surgical resection is virtually impossible due to the invasive growth of GBM in vital regions of the brain [2]. Treatment is also considered ineffective because GBM is also highly heterogeneous, both in terms of temporal heterogeneity and spatial heterogeneity [3–5]. Temporal heterogeneity mainly refers to the evolution of secondary GBMs [6], while spatial heterogeneity refers to intratumoral variation, such as necrotic and invasive areas, which have their own molecular and biological characteristics [7]. The presence of so-called glioma stem cells is also an indication of spatial heterogeneity. For these reasons, drug treatment is still a very important part of the treatment strategy, and multidrug cocktail therapy may become the standard for GBM treatment in the future [8, 9].

The development of new drugs is a time-consuming, costly, and failure-prone business venture. However, the current dilemma in antibiotic research has forced us to consider the long-term sustainability of new drug development [10–12]. To date, more than 30 million compounds have been discovered by humans, some of which have been used as drugs. Drug repurposing, which refers to the identification of new indications for already approved drugs, offers promising options to overcome the problems of drug development [13,14]. The reduction in the incidence of cancer in schizophrenic patients taking antipsychotic drugs has attracted the attention of researchers [15, 16].

Current research suggests that antipsychotic drugs bind to different receptors, such as the dopamine receptor (DR), muscarinic M1 receptor, adrenergic alpha receptor,

5-hydroxytryptamine (5-HT) receptor, and histamine H1 receptor, to produce therapeutic effects.

Traditional antipsychotic drugs such as fluspirilene, perphenazine, and sulpiride have been used in the treatment of schizophrenia [17]. Using both bioinformatics and biological experiments, previous studies have reported that fluspirilene, perphenazine, and sulpiride possess potent antitumor activity [18–21]. In particular, fluspirilene has been shown to inhibit glioma stem cells [22]. However, its antitumor mechanism remains unclear. The drug is a highly attractive candidate for repurposing in the treatment of GBM due to its inherent blood-brain barrier permeability. In the present study, we investigated its potential as a therapy for GBM both *in vitro* and *in vivo* and identified critical molecular players underlying its antitumor activity.

## Materials and methods

**Cell culture and reagents.** All experimental protocols were approved by the Research Ethics Committee of Qingdao University and performed according to the relevant provisions. Human glioma cell lines (U87MG, U251, and LN229) were obtained from the Cell Bank of the Chinese Academy of Sciences (Shanghai, China). U87MG, U251, and LN229 cells were cultured in Dulbecco's modified Eagle's medium (DMEM; Thermo Fisher Scientific, USA) supplemented with 10% fetal bovine serum (FBS; Thermo Fisher Scientific). Human primary GBM cells, GBM#P3, were kindly provided by Professor Rolf Bjerkvig, Department of Biomedicine, University of Bergen, Norway. GBM#P3 cells were cultured in Neurobasal Medium (Thermo Fisher Scientific) supplemented with B27 Neuro Mix (20 µl/ml), FGF (20 ng/ml), and EGF (20 ng/ml; Thermo Fisher Scientific). All cells were maintained at 37 °C in a humidified incubator containing 5% $CO_2$. Fluspirilene (1841-19-6), perphenazine (58-39-9), and sulpiride (15676-16-1) were purchased from TOPSCIENCE (Shanghai, China). All the aforementioned drugs were diluted with 0.1% dimethyl sulfoxide (DMSO; Thermo Fisher Scientific) and stored frozen. When needed, they are thawed and mixed with cell culture medium to the preset concentrations (0, 20, 40, 60, and 80 µM) and used to replace the original culture medium for treating the cells. In another experiment, DMSO of the same concentrations as the preset drug concentrations is chosen as the control group.

**Gene Ontology (GO) and protein interaction network analysis.** L1000 Fireworks Display (L1000FWD; http://amp.pharm.mssm.edu/l1000fwd/) is a user-friendly database that provides interactive visualization of over 16,000 drug- and small-molecule-induced transcriptome signatures [23]. In this study, we used the L1000FWD database to query the expression changes in several tumor cell lines treated with fluspirilene. Genes that were most significantly downregulated and consistently altered across cell lines were selected as target genes for experimental verification. GO enrichment analysis was performed using DAVID (http://david.abcc.ncifcrf.gov/home.jsp) to explore the possible biological processes involved [24]. mRNA and protein expression data were obtained from TCGA [25], GEO (https://www.ncbi.nlm.nih.gov/geo/) [26], and Human Protein Atlas (HPA; https://www.proteinatlas.org/) databases [27]. Analysis of genes correlated with target genes was performed using TCGA GBM (http://cancergenome.nih.gov) and Rembrandt (https://caintergator.nci.nih.gov/rembrandt) datasets [28]. Protein interaction network analysis was performed using the String database (https://string-db.org/).

**Cell viability assay.** All experimental protocols were approved by the Research Ethics Committee of Qingdao University and performed according to the relevant provisions. Cell viability was assessed using the Cell Counting Kit-8 (Dojindo, Kumamoto, Japan) according to the manufacturer's instructions. Briefly, cells ($3\times10^3$) were seeded into 96-well plates and allowed to attach overnight. After treatment, absorbance (450 nm) was measured using the CCK-8 assay in an EnSight Multimode Plate Reader (PerkinElmer; Singapore). $IC_{50}$ represents the concentration at which a substance exerts half of its maximal inhibitory effect. The $IC_{50}$ values were calculated using GraphPad Prism version 8 software (San Diego, CA, USA).

**5-ethynyl-2'-deoxyuridine (EdU) cell proliferation assay.** GBM cells ($2\times10^4$) were seeded in 24-well plates, allowed to adhere, and treated. After treatment, cell proliferation was measured using the EdU Apollo 567 Cell Tracking Kit (Ribo-bio; Guangzhou, China). Briefly, cells were incubated with EdU reagent (200 µM) for 2 hours at room temperature, fixed with 4% paraformaldehyde for 20 minutes, and permeabilized with 0.5% Triton X-100 for 10 minutes. Cells were rinsed three times with phosphate-buffered saline (PBS), incubated with 100 µl Apollo reagent for 30 min, and stained with 4',6-diamidino-2-phenylindole (DAPI). Three fields of view were randomly selected for counting EdU-positive cells and three independent experiments were performed.

**Cell colony formation assay.** Pretreated GBM cells (500 cells per well) were seeded in six-well plates and cultured for 2 weeks. The complete medium was replaced twice a week. After 2 weeks, cells were fixed and stained with 100% methanol and 5% crystal violet, and colonies (≥50 cells) were counted. Statistical data were obtained from three independent experiments.

**Mitochondrial membrane potential assay (JC-1).** The mitochondrial membrane potential assay was performed according to the manufacturer's protocol (Beyotime; Shanghai, China). The indicator dye for measuring mitochondrial membrane potential in treated cells was detected using a laser scanning confocal microscope (Leica SP8; Leica, Solms, Germany).

**Flow cytometry.** Apoptosis was detected using the Annexin V-FITC/PI Apoptosis Detection Kit (BD Biosciences, San Jose, CA, USA). After treatment, U87MG and U251 cells were digested, harvested, and stained with Annexin V-FITC/PI reagent for 20 min. Apoptosis assays

were analyzed using the flow cytometer CytoFLEX (Beckman Coulter; Brea, CA, USA).

Cell cycle distribution was determined by propidium iodide (PI; BD Biosciences; San Jose, CA, USA) staining of DNA. Cell cycle assays were analyzed using a C6 flow cytometer (BD Biosciences, San Jose, CA, USA). Experimental results were analyzed using Flowjo software (Tree Star; Ashland, OR, USA).

**Western blotting.** The treated cells were lysed for 30 min in RIPA buffer (Thermo Fisher Scientific) supplemented with the protease inhibitor phenylmethanesulfonyl fluoride (PMSF, Beyotime; Shanghai, China). Protein lysates (20 μg) were separated by 10% sodium dodecyl sulfate-polyacrylamide gel electrophoresis (SDS-PAGE) and transferred to polyvinylidene difluoride (PVDF) membranes (0.22 μm, Merck Millipore; Darmstadt, Germany). Membranes were blocked for 1 h at room temperature in Tris-buffered saline with Tween-20 (TBST, 10 mM Tris, 150 mM NaCl, and 0.1% Tween-20) containing 5% skimmed milk powder (BSA; Beyotime; Shanghai, China). Strips were incubated with primary antibody at 4 °C overnight, followed by incubation with horseradish peroxidase (HRP)-conjugated secondary antibody dissolved in antibody dilution buffer (Beyotime; Shanghai, China; dilution 1:5000) for 1 h at room temperature. Specific proteins were visualized by enhanced chemiluminescence (ECL, Millipore; Bedford, MA, USA) according to the manufacturer's protocol. The following primary antibodies were used KIF20A (D-3; Santa Cruz Biotechnology; Dallas, TX, USA), FOXM1 (D12D5; Cell Signaling Technology; Danvers, MA, USA), and GAPDH (10494-1-AP; Proteintech; Wuhan, China). All western blotting experiments were repeated more than three times. Quantitative analysis of western blot images used the ImageJ software (the National Institutes of Health; Bethesda, MD, USA).

**Real-time quantitative PCR (RT-qPCR).** Total RNA was isolated from GBM cells using the RNA-Quick Purification Kit (Shanghai YiShan Biotechnology; Shanghai, China) according to the manufacturer's protocol. cDNA was synthesized from total RNA (2 μg) using the ReverTra Ace qPCR RT Master Mix Kit (FSQ-101; TOYOBO, Osaka, Japan) and used as a template in real-time fluorescence quantification. RT-qPCR was performed with SYBR Green Master Mix (Roche; Basel, Switzerland) on the Real-Time PCR Detection System (Roche 480II). Experiments were conducted in triplicate, and *GAPDH* served as an internal control. The following were used: *BIRC5*: F 5'-TTTCTCAAGGACCACCGCATC-3', R 5'-CAAGTCTGGCTCGTTCTCAG-3'; *FOXM1*: F 5'-GCTTGCCAGAGTCCTTTTTG-3', R 5'-CCACCTGAGTTCTCGTCAATGC-3'; *GAPDH*: F 5'-ACCCACTCCTCCACCTTTGAC-3', R 5'-TGTTGCTGTAGCCAAATTCGTT-3'; *HN1L*: F 5'-CCCAGGAGGAGAATCGAGCA-3', R 5'-CGGGGGTTGATTCGTCAAAG-3'; *KIF2C*: F 5'-CAGTGGAATGGGCAGAAGGA-3', R 5'-CGGGCAAATTCCCAGTTTGG-3'; *KIF20A*: F 5'-GCCAACTTCATCCAACACCT-3', R 5'-GTGGACAGCTCCTCCTCTTG-3'; *MALT1*: F, 5'-GATGCGTAATGCTGTGGATG-3'; R 5'-GGTATCATCGTAGTCATTTCTTTTTCC-3'.

**Gene silencing and ectopic expression.** Small interfering RNAs (siRNA; GenePharma; Shanghai, China) were transfected into cells with Lipofectamine 2000 (Invitrogen/Thermo Fisher Scientific) according to the manufacturer's protocol. Knockdown efficiency was evaluated 48 h after transfection with RT-qPCR and western blotting. siRNA sequences (n=2) that generated efficient knockdown were the following: Si-KIF20A-1: 5'-GUUCUCAGCCAUUGCUAGCTT-3'; Si-KIF20A-2: 5'-CCGUUCCUGCAUGAUUGUCAA-3'; Negative control: 5'-UUCUCCGAACGUGUCACGUTT-3'; Si-FOXM1-1: 5'-GCUGGGAUCAAGAUUAUUATT-3'; Si-FOXM1-2: 5'-UGGUUAAUAAUCUUGAUCCCA-3'; Negative control: 5'-UUCUCCGAACGUGUCACGUTT-3'.

**Orthotopic xenograft model.** All animal surgical interventions and post-operative animal care were approved by The Institutional Animal Care and Use Committee (IACUC) of Qingdao University (QDYHD-2022-0476). U87MG cells infected with lentivirus expressing luciferase-GFP ($3\times10^5$; OBiO Technology; Shanghai, China) were stereotactically implanted into the brains of 4-week-old athymic mice. After 7 days, tumor size was determined and animals were divided into the following 2 groups: control (n=6) and fluspirilene (n=6). Mice were administered diluted DMSO (control) or fluspirilene (4 mg/kg) by intramuscular injection every other day. Tumour volume was monitored by bioluminescence imaging (PerkinElmer IVIS Spectrum; Waltham, MA, USA). At the end of the experiment, tumors were dissected and snap-frozen in liquid nitrogen or fixed in formalin for further analysis. All animal surgical interventions and post-operative animal care were approved by The Institutional Animal Care and Use Committee (IACUC) of Qingdao University (QDYHD-2022-0476).

**Immunohistochemistry (IHC).** The xenograft specimen was excised, fixed in formaldehyde, embedded in paraffin, and sectioned (4 μm). After dewaxing and rehydration, epitope retrieval was performed on the sections for 20 minutes (10 mM citric acid buffer, pH 7.2, 95 °C). After cooling, the slides were incubated with primary antibodies (rabbit anti-FOXM1 1:200 dilution, mouse anti-KIF20A 1:50 dilution) at 4 °C overnight. The next day, the primary antibody was removed and the HRP-conjugated secondary antibody was added and incubated for 1 h at room temperature. Target proteins were detected using diaminobenzidine (DAB, Beyotime; Shanghai, China) and slides were counterstained with hematoxylin (Beyotime; Shanghai, China).

**Plotting and statistical analysis.** Each assay was performed at least three independent times. Data analysis was performed using GraphPad Prism version 8 software. Data were expressed as mean ± SD. We followed the methods of Kong et al. [29]. The statistical significance of experimental data was assessed using Student's t-test (two-tailed) between two groups. One-way analysis of variance (ANOVA) was

used to compare more than two groups. For sequencing data in a common database, non-parametric tests were used to detect differences. Differences were considered significant at the following p-values: *p<0.05; **p<0.01; ***p<0.001.

## Results

**Identification of fluspirilene as an anti-GBM drug for further exploration.** As mentioned in the preface, fluspirilene, perphenazine, and sulpiride have been reported to have strong antitumor activity. Although fluspirilene belongs to the butyrophenone antipsychotics, perphenazine, and sulpiride belong to the phenothiazine antipsychotics. However, they have anti-schizophrenic activity and similar molecular weights of 475.6 g/mol, 404.0 g/mol, and 341.4 g/mol respectively (Figures 1A–C). Cells were treated with a fixed dose interval of the drug (0, 20, 40, 60, 80 μM) and analyzed for remaining viable cells after 24 h and 48 h. Growth curves generated with the CCK-8 assay showed that the viability of GBM cell lines decreased with increasing concentrations of fluspirilene, perphenazine, and sulpiride. The $IC_{50}$ values of fluspirilene were 37.8 μM, 41.5 μM, 39.8 μM, and 34.6 μM at 24 h for U87MG, U251, LN229, and GBM#P3 cells, respectively (Figure 1D). The cell viability curve of fluspirilene was more consistent at 48 h (Figure 1G). Compared to fluspirilene, the inhibition of cell viability by perphenazine was significantly weaker, with $IC_{50}$ values of 124.4 μM, 116.1 μM, 98.8 μM, and 54.6 μM at 24 h for U87MG, U251, LN229, and GBM#P3 cells, respectively (Figure 1E). The inhibitory effect of sulpiride was the least significant (Figure 1F). The above

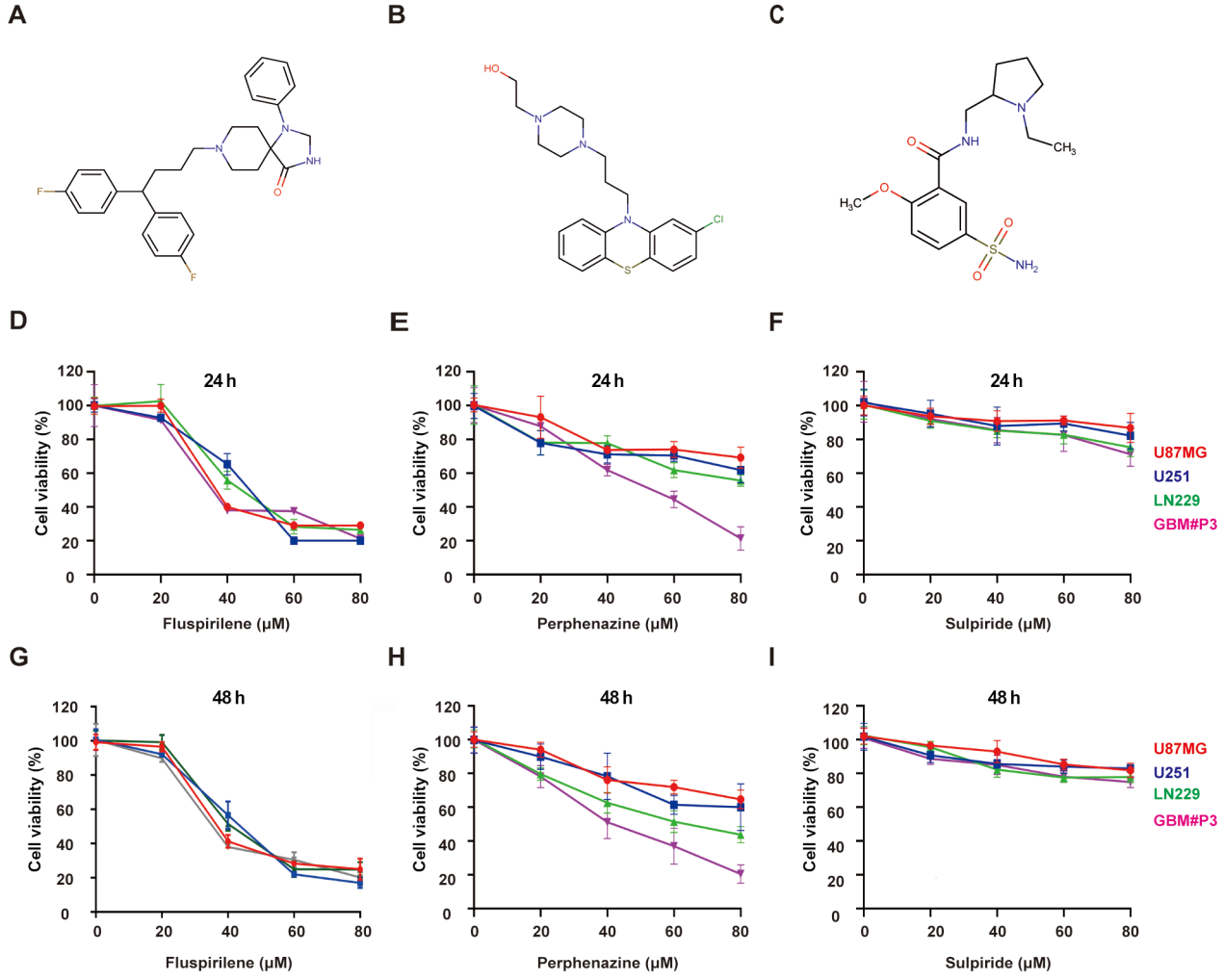


**Figure 1. Fluspirilene, perphenazine, and sulpiride inhibit GBM cell viability. A–C) Molecular structure of fluspirilene, perphenazine, and sulpiride. Graphic representation of results from the CCK-8 assay to determine cell viability of U251, U87MG, LN229, and GBM#P3 cells treated with different concentrations of fluspirilene for 24 h (D) and 48 h (G). Graphic representation of results from the CCK-8 assay to determine cell viability of U251, U87MG, LN229, and GBM#P3 cells treated with different concentrations of perphenazine for 24 h (E) and 48 h (H). Graphic representation of results from the CCK-8 assay to determine cell viability of U251, U87MG, LN229, and GBM#P3 cells treated with different concentrations of sulpiride for 24 h (F) and 48 h (I). Data points are the percentage (%) relative to untreated cells at the same time point.**

inhibitory effect of perphenazine and sulpiride is relatively stable at 48 h as shown in Figures 1H and I. Therefore, fluspirilene was designated as a target for further exploration.

**Fluspirilene inhibits the proliferation of GBM cells.** GBM cells were treated with different concentrations of fluspirilene *in vitro* and growth was assessed in two different assays. EdU incorporation in fluspirilene-treated U87MG and U251 cells both decreased in a dose-dependent manner (~80% and 82%, respectively, at 40 μM; Figures 2A–D). The colony formation assay is an effective method to assess the proliferative capacity of single cells. In the colony formation assay, the number of colonies gradually decreased with increasing drug concentration. The above results showed that fluspirilene inhibited the proliferation of human GBM cell lines (~75% and 80, respectively, at 30 μM; Figures 2E and 2F).

**Fluspirilene-induced GBM cells' apoptosis *in vitro*.** Next, we investigated whether growth suppression mediated by fluspirilene induces apoptosis in GBM cells. U87MG and U251 cells were treated with different concentrations of fluspirilene (0, 20, and 30 μM). We first determined whether we could detect early stages of apoptosis by changes in mitochondrial membrane potential. After 12 h, a diluted JC-1 probe, which changes color upon accumulation in mitochondria, was incubated with GBM cells and the red/green fluorescence intensity ratio was calculated to detect mitochondrial membrane potential ($\Psi_m$). The decreasing

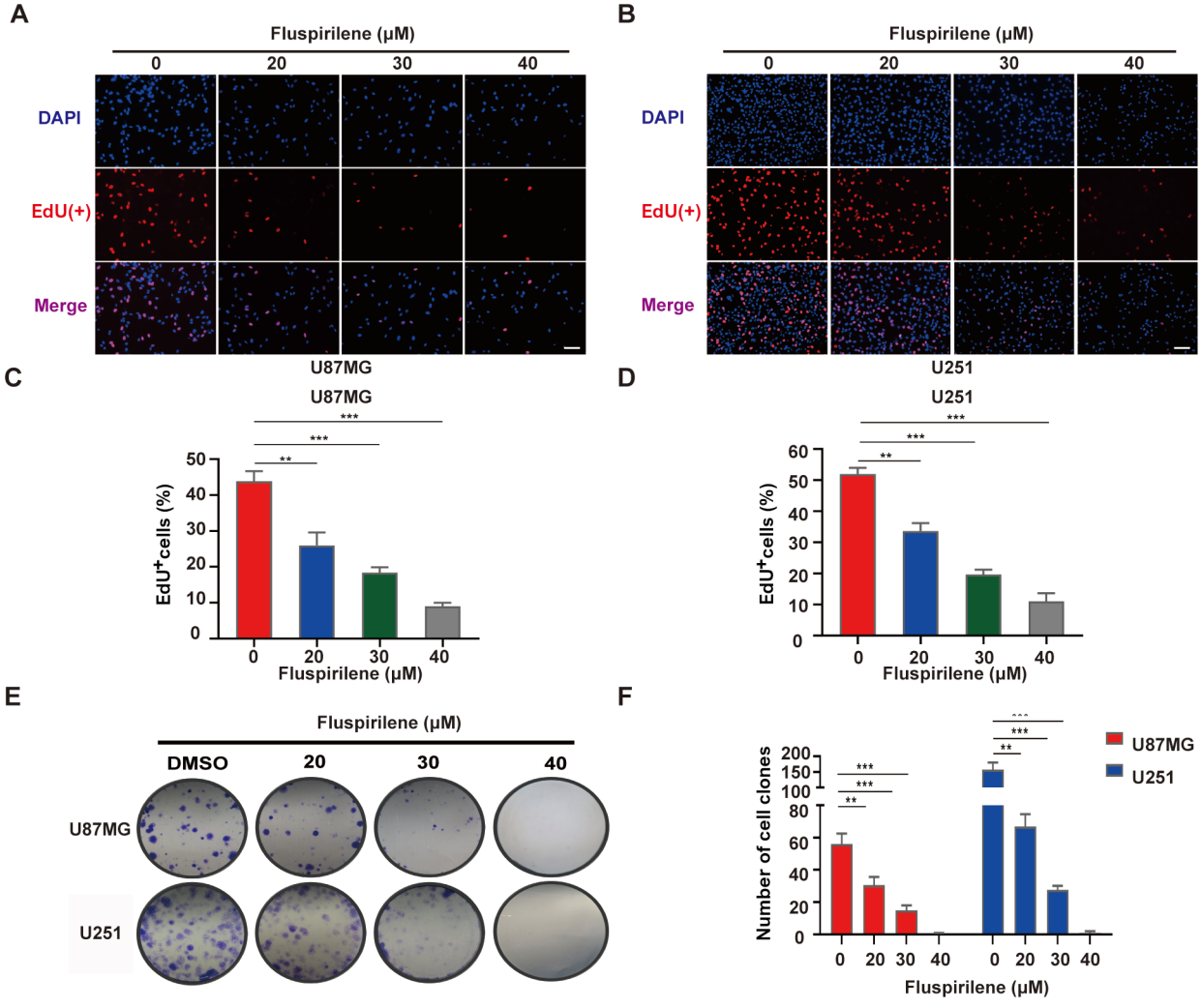


**Figure 2. Fluspirilene inhibits the proliferation of GBM cells. Fluorescence images of EdU incorporation in U87MG (A) and U251 (B) cells treated with fluspirilene or DMSO for 24 h. Cells were stained with Apollo 567 (red) to detect EdU and DAPI (blue) to highlight nuclei, and images were merged (scale bars: 100 μm). Graphic representation of the percentage of EdU+ U87MG (C) and U251 (D) cells treated with different concentrations of fluspirilene for 24 h. The percentage of EdU+ cells (EdU positive/DAPI positive × 100%) was determined in 3 random fields per sample. E) Representative images of colony formation assays for U87MG and U251 after treatment with the indicated concentrations of fluspirilene for 2 weeks. F) Graphic representation of the results from colony formation assays for U87MG and U251 cell lines under treatment with different concentrations of fluspirilene. **p<0.01; ***p<0.001 compared to control.**

relative ratios with the increasing drug showed that fluspirilene reduced the mitochondrial membrane potential and induced mitochondrial apoptosis (Figure 3A and Figure 3B). Annexin V-FITC and PI staining of treated cells confirmed these results. Flow cytometric analysis showed that the proportion of cells in the early and middle stages of apoptosis was significantly and dose-dependently increased in fluspirilene-treated GBM cells compared to controls (22.05% and 37.39%; 32.89% and 46.04% in U87MG and U251 cell lines, respectively; Figure 3C).

**Bioinformatics analysis of the anti-GBM effect of fluspirilene.** As fluspirilene is an anti-schizophrenic drug currently in clinical use, many microarray studies have been performed on various tumor cell lines, including MCF-7, VCaP, PC3, HCC515, and A549 cells treated with the drug. We identified a total of 1,309 differentially expressed genes (DEGs; |fold change| >1.5, p-value <0.05) from these data and generated a heat map with the expression profiles of the top 50 DEGs (Figure 4A). The 8 DEGs that showed the most significant decrease in expression across cell lines in response to the drug were as follows: *KIF20A, CCNB2, DPH2, TCEGR1, GTF2A2, BIRC5, MYCBP,* and *NUP88*. GO enrichment analysis was performed to gain insight into the molecular function of the DEGs. Upregulated genes were mainly enriched in processes such as small molecule biosynthesis, regulation of cellular stress response, and negative regulation of protein modification. Downregulated genes were mainly enriched in molecular function processes, including cell cycle regulation, cell division, positive regulation of cell death, the cell cycle of G2/M phase transition, and microtubule cytoskeleton organization involved in mitosis (Figure 4B). These results suggest that fluspirilene

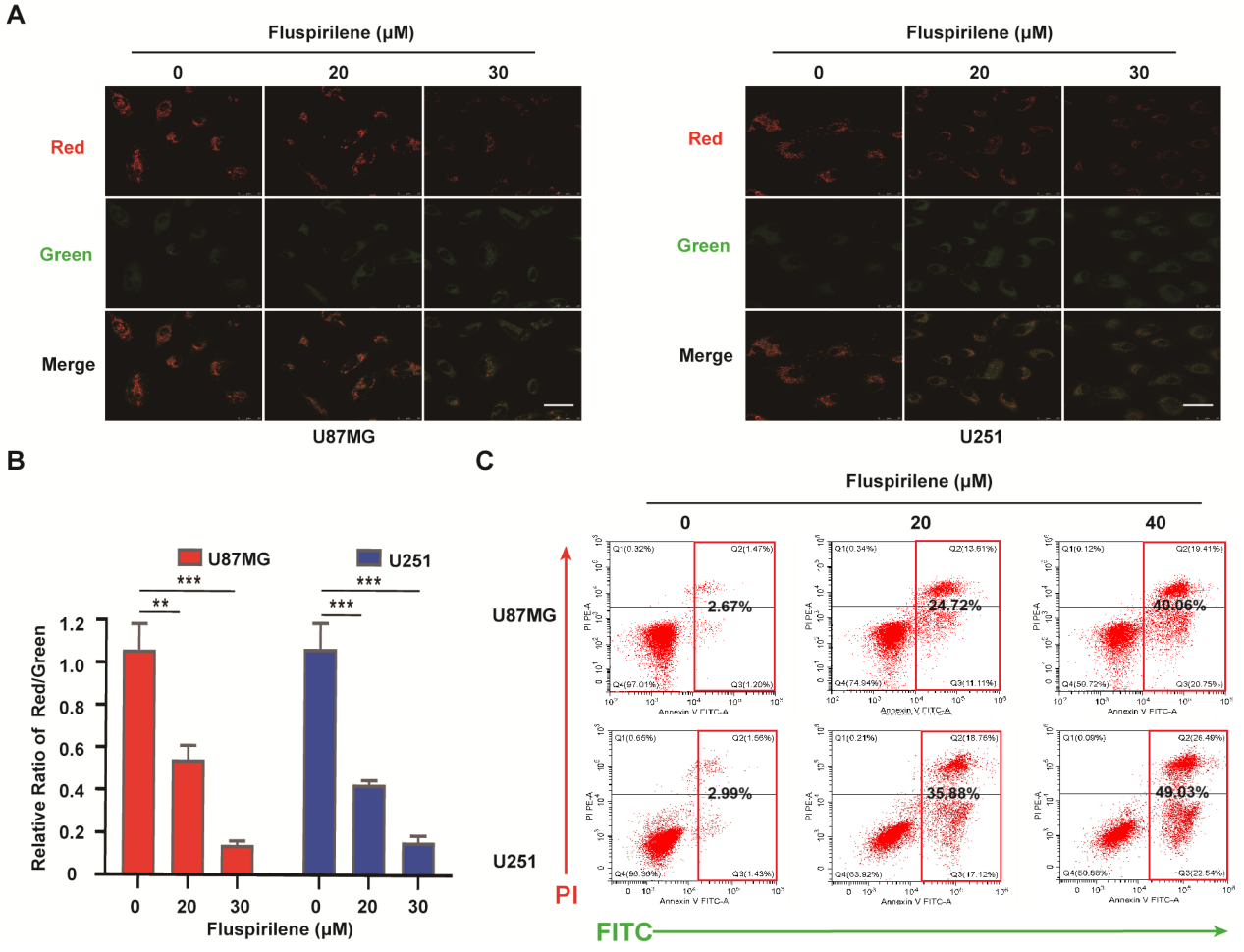


**Figure 3. Fluspirilene induces mitochondrial apoptosis of GBM cells. A) Fluorescence images of mitochondrial membrane potential assay in U87MG and U251 cells treated with fluspirilene or DMSO for 24 h. Red fluorescence represents J-aggregates, indicating a high mitochondrial potential. Green fluorescence represents monomers and a low mitochondrial potential. B) Graphic representation of the relative ratio of red/green fluorescence from A. in U87MG and U251 treated with DMSO or fluspirilene (20 μm and 30 μm) for 24 h. C) Flow cytometric analysis of AnnexinV-FITC and PI staining for the determination of apoptosis in U87MG and U251 cells after treatment with DMSO or corresponding concentrations of fluspirilene for 24 h. **p<0.01; ***p<40.001 compared to control.**

may inhibit tumor progression by downregulating genes involved in these biological processes.

**Identification of fluspirilene target gene in GBM cells.** To understand the molecular mechanisms mediating its antitumor effect, we focused on DEGs downregulated under fluspirilene treatment. We chose to validate a subset of these DEGs, those showing the most significant decrease in expression, *KIF20A, KIF2C, HN1L, MALT1, and BIRC5*, in our GBM cell lines. We treated GBM cells (U87MG, U251, and GBM#P3) with fluspirilene (20 μm) for 24 h, extracted total RNA, and performed RT-qPCR. The experimental results showed that only *KIF20A* was downregulated in all three GBM cell lines (Figure 4C). Immunoblotting confirmed these results (Figure 4D). Based on these results, *KIF20A* was identified as a target gene for the anti-GBM effects of fluspirilene.

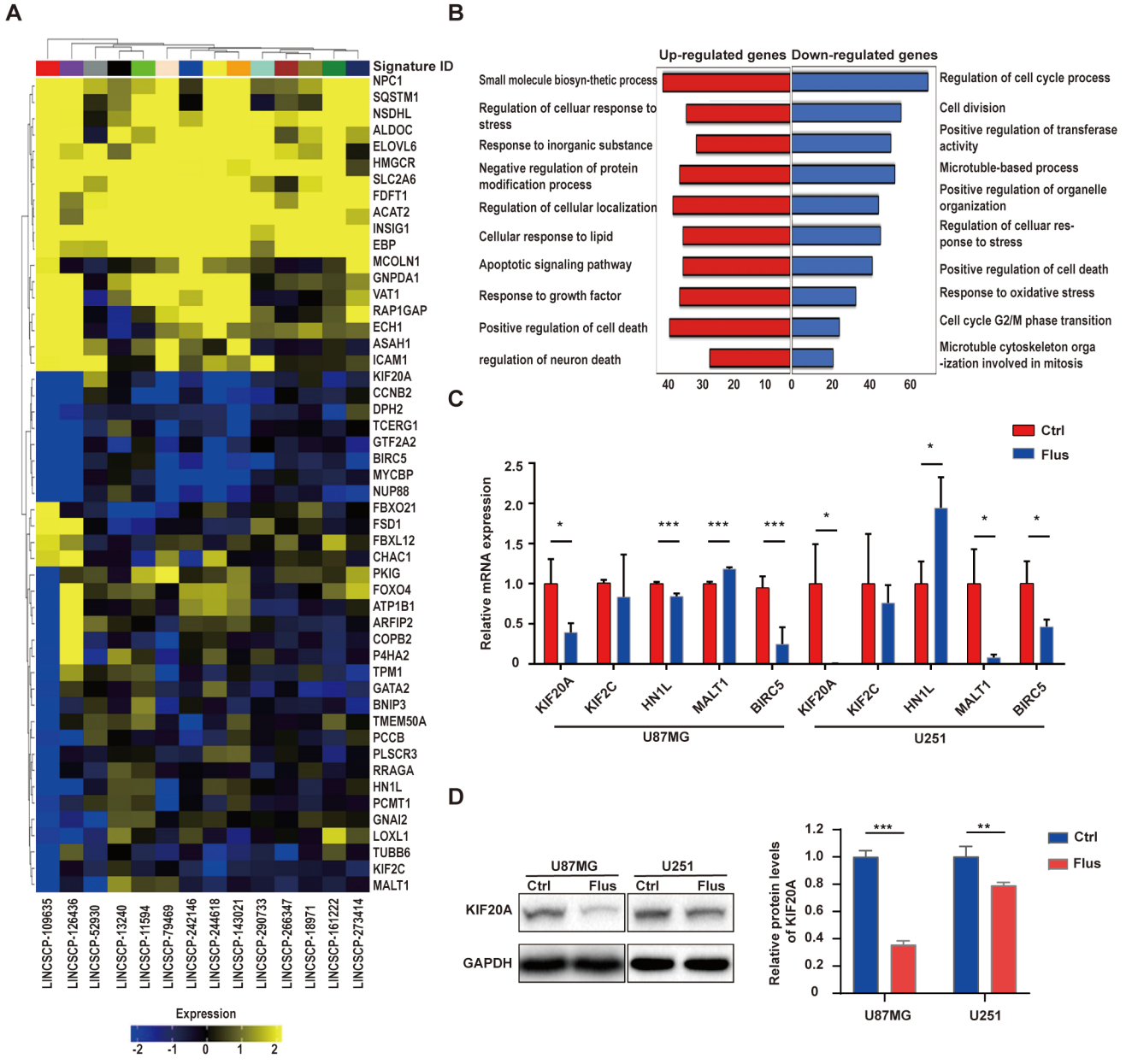


**Figure 4. Fluspirilene reduces the expression of KIF20A. A) Cluster heat map of the top 50 DEGs in multiple tumor cell lines treated with fluspirilene. B) Gene Oncology (GO) enrichment analysis showing potential biological processes of all DEGs. C) Real-time quantitative PCR results for *KIF20A*, *KIF2C*, *HN1L*, *MALT1*, and *BIRC5* after treatment with fluspirilene (20 μM) in U87MG and U251 cell lines. GAPDH was used as an internal reference. D) Western blots for KIF20A after treatment of U87MG and U251 cell lines fluspirilene (20 μM). GAPDH was used as the protein loading control. *p<0.05; ***p<0.001 compared to control.**

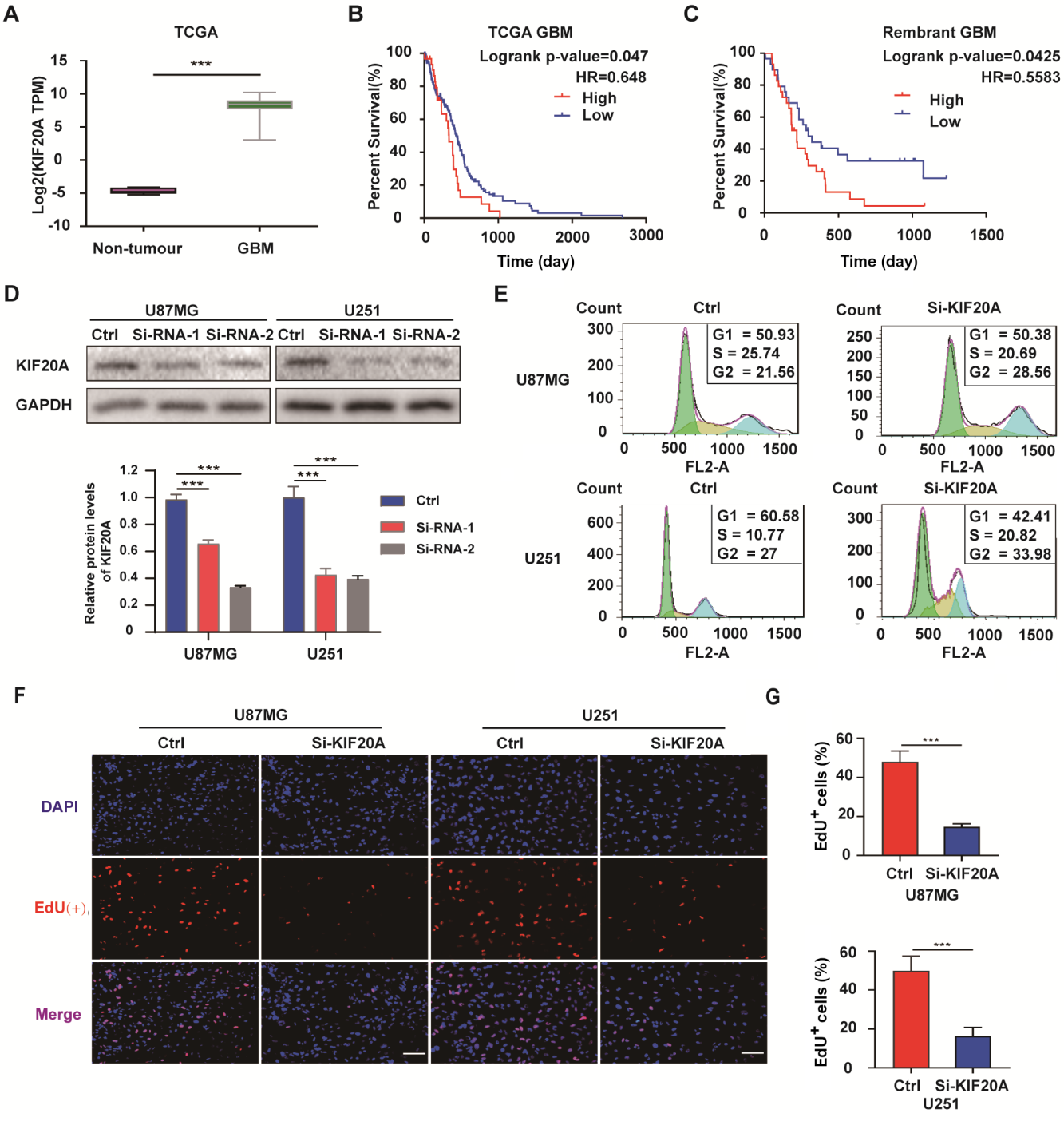


**Figure 5. Inhibition of KIF20A suppresses cell growth in GBM cells. A) Graphic representation of the mRNA expression of *KIF20A* in GBM in TCGA database. Kaplan–Meier survival curves for patients with GBM KIF20A high and GBM KIF20A low from TCGA (B) and Rembrandt databases (C). D) Western blot to validate the efficiency of si-KIF20A in U87MG and U251 cell lines. GAPDH was used as a protein loading control. E) Flow cytometry showing cell cycle parameters after siRNA knock-down of KIF20A in U87MG and U251 cell lines. F) Fluorescence images of EdU incorporation in U87MG and U251 cells treated with DMSO or fluspirilene for 48 h. Cells were stained with Apollo 567 (red) to detect EdU and DAPI (blue) to highlight nuclei, and images were merged (scale bars: 100 μm). G) Graphic representation of the percentage of EdU positive cells (EdU positive/DAPI positive × 100%) in U87MG and U251 after siRNA knockdown of KIF20A. *p<0.05; **p<0.01; ***p<0.001 compared to control.**

**A small molecule targeting KIF20A inhibits the growth of GBM cells *in vitro*.** The expression levels of KIF20A, a member of the kinesin family, are significantly higher in GBM than in normal tissue based on array data in TCGA dataset (Figure 5A). The survival time of GBM *KIF20A*$^{high}$ patients was also significantly shorter than that of GBM *KIF20A*$^{low}$ patients (Figures 5B and 5C). Immunohistochemistry results in the HPA database also showed that KIF20A levels were elevated in human gliomas compared to non-neoplastic brain tissue, with GBM showing the highest levels (GBM > LGG > normal tissue; Figure S1A).

We therefore used siRNA knockdown to determine whether KIF20A has a growth-promoting role in human glioma. RT-qPCR and western blotting were performed to confirm the knockdown efficiency of the siRNAs in U87MG and U251 cells (Figure 5D, Figures S1B and S1C). Previous studies have shown that KIF20A regulates mitosis and cytokinesis [30, 31]. We therefore examined cell cycle kinetics and EdU incorporation. Flow cytometry showed that GBM cells accumulated in the G2/M phase after KIF20A knockdown in U87MG and U251 cells compared to controls (an increase of 7% and 6.98%, respectively; Figure 5E). EdU incorporation was also reduced by KIF20A knockdown in both U87MG and U251 cell lines (Figure 5F).

**Fluspirilene inhibits the proliferation of GBM cells by suppressing the FOXM1-KIF20A axis.** The String database is currently the largest protein interaction database available and collects a large number of protein-regulatory relation-

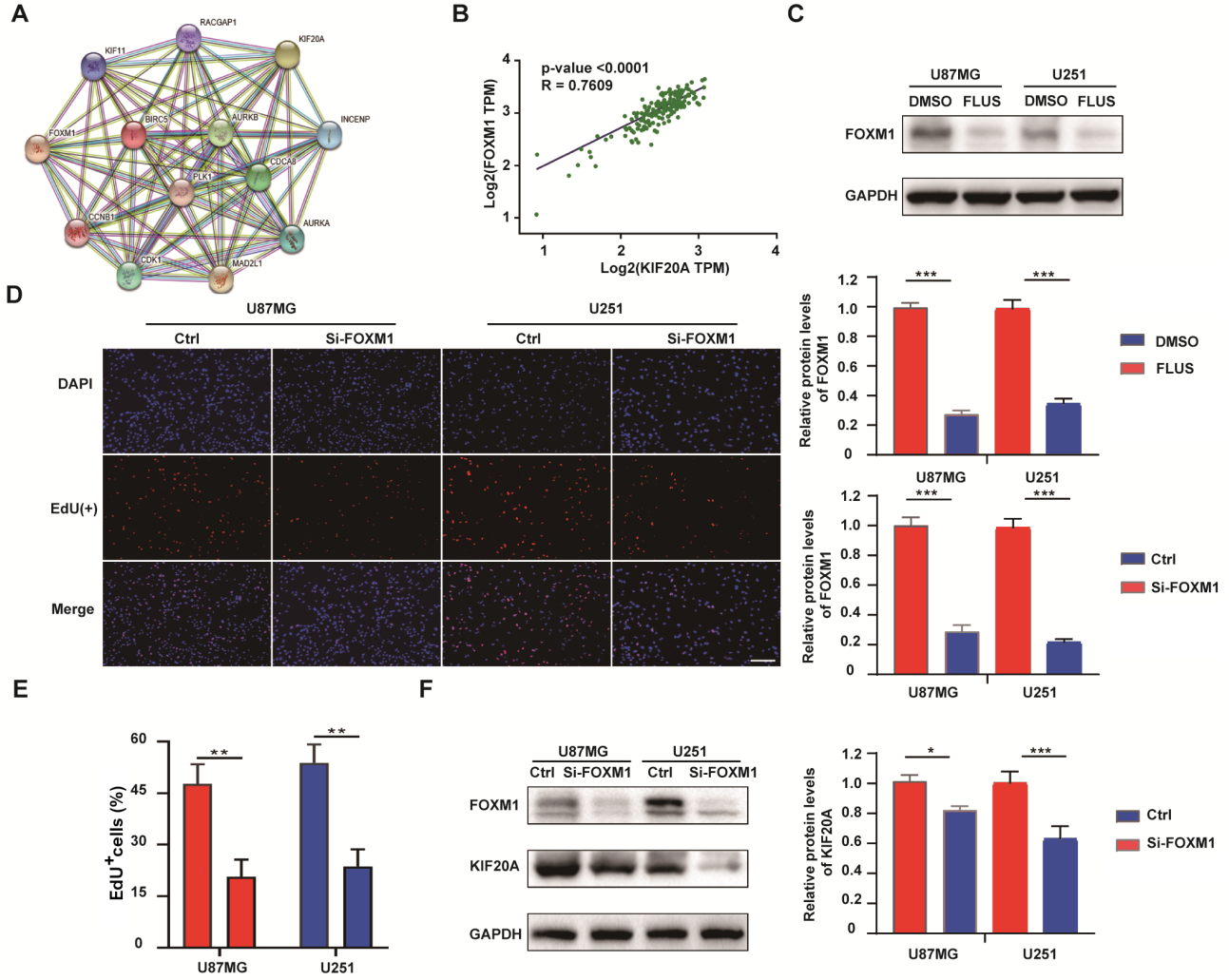


**Figure 6. Fluspirilene exerts anti-GBM activity by suppressing the FOXM1-KIF20A axis. A) Protein-protein interaction network. B) Based on TCGA database, the mRNA expression levels of FOXM1 were positively correlated with KIF20A. C) Western blot showing FOXM1 levels in U87MG and U251 cells after treatment with fluspirilene (20 μM). GAPDH was used as the protein loading control. D) Fluorescence images of EdU incorporation in U87MG and U251 cells treated with DMSO or fluspirilene for 48 h. Cells were stained with Apollo 567 (red) to detect EdU and DAPI (blue) to highlight nuclei, and images were merged (scale bars: 100 μm). E) Fluorescence images of EdU incorporation and statistical results from U87MG and U251 cells after siRNA knockdown of FOXM1. F) Western blot to evaluate KIF20A levels after siRNA knockdown of FOXM1. GAPDH was used as a protein loading control. *p<0.05; **p<0.01; ***p<0.001 compared to control.**

ships that have been experimentally verified or based on biological predictions. When KIF20A was entered into the String database, we obtained a regulatory network that included *AURKA, AURKB, BIRC5, INCENP, CDCA8, KIF11, CDK1, CCNB1,* and *PLK1* (Figure 6A). The genes in this network are closely associated with the cell cycle and cell division. FOXM1 is a well-known oncogenic transcription factor that affects cell proliferation by regulating cell cycle-associated proteins. At the mRNA expression level, we found that FOXM1 and KIF20A showed significant correlations in TCGA GBM dataset (Figure 6B). Many studies have also reported that FOXM1 can regulate KIF20A at the transcriptional level. Compared to normal tissues, the expression level of FOXM1 at both mRNA and protein levels was significantly increased in TCGA database compared to non-neoplastic brain tissues or low-grade gliomas (Figures S2A and S2B).

To determine whether fluspirilene alters the expression of FOXM1, we examined the mRNA and protein levels of the transcription factor in U87MG and U251 cells treated with the drug at 30 μM for 48 h. The expression of FOXM1 decreased at the protein level in both U87MG and U251 cells (Figure 6C). To verify the regulation of KIF20A by FOXM1, siRNA was used to knock down FOXM1. RT-qPCR and western blotting confirmed the knockdown efficiency of the siRNAs (Figures S2C and S2D). Cell growth was reduced in both U87MG and U251 cells as assessed by EdU incorporation (Figure 6D). At the molecular level, FOXM1 knockdown resulted in decreased KIF20A protein levels (Figure 6F).

**Fluspirilene inhibits the growth of GBM cells *in vivo*.** To investigate the efficacy of fluspirilene, we established an orthotopic xenograft model in mice using luciferase-expressing U87MG cells and compared tumor devel-

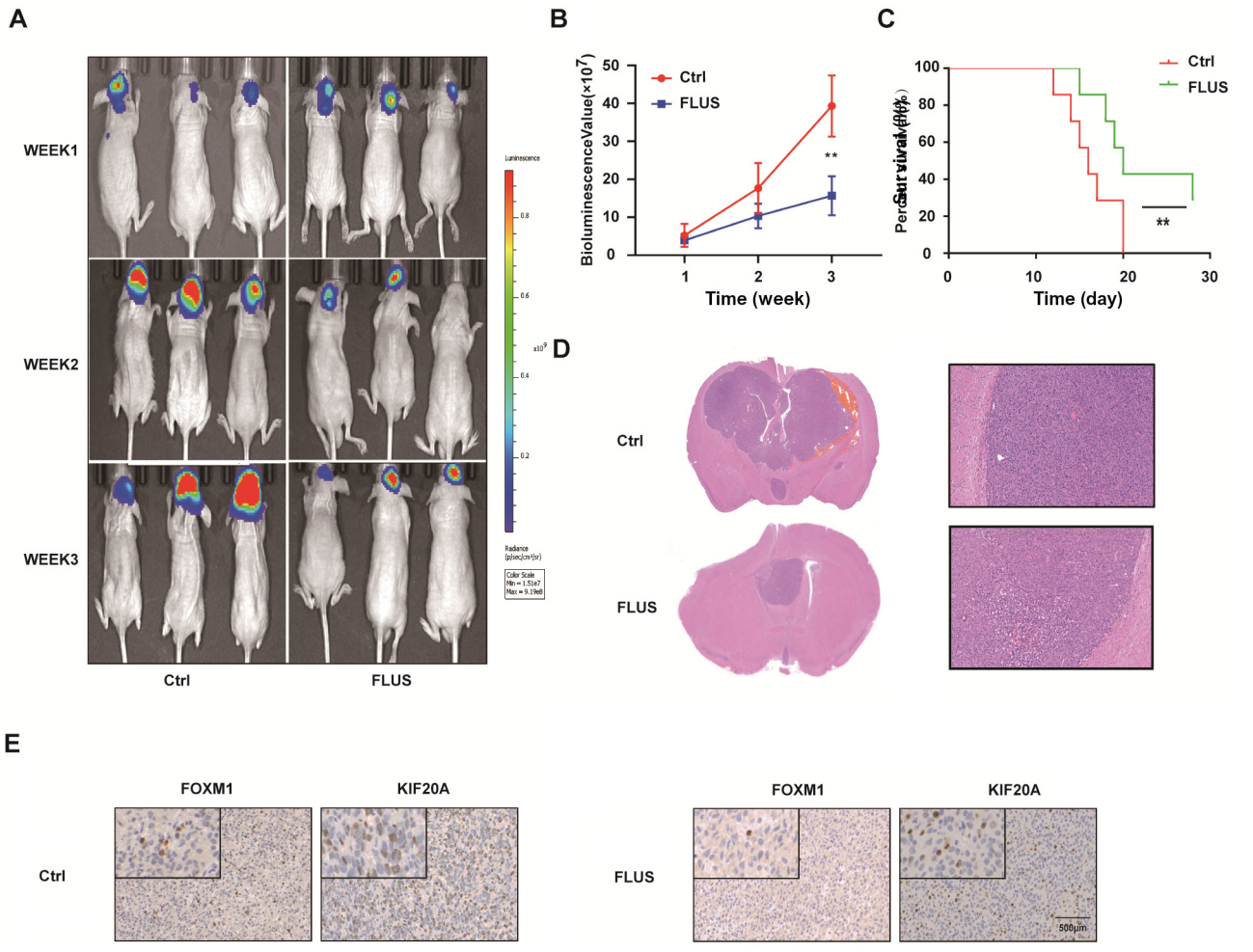


**Figure 7. Fluspirilene inhibits the growth of GBM cells *in vivo*. A) Luciferase-stable U87MG cells were orthotopically implanted into athymic nude mice, and tumor growth was monitored using the PerkinElmer IVIS Spectrum imaging system for detection of bioluminescence. Bioluminescent signals were measured at weeks 1, 2, and 3 after implantation. B) Bioluminescence values plotted as a function of time in days to assess tumor growth (weeks 1, 2, and 3). C) Kaplan-Meier survival curves for animals implanted with tumor cells and treated with drug. A log-rank test was used to assess the statistical significance of the differences. D) Representative image of HE staining of tumor specimens. E) Images of IHC staining for KIF20A and FOXM1 in tumors from each group as indicated (scale bars: 500 μm). **p<0.01 compared to control.**

opment in treated animals with controls. Fluorescence signal intensity in drug-treated animals did not increase as rapidly over time as in controls (at 3 weeks, ~$37.8\times10^7$ vs ~$15.3\times10^7$ photons/s, fluspirilene vs. control; Figures 7A and 7B). The survival time of treated mice was also significantly prolonged compared to control mice (20 weeks vs 16 weeks; Figure 7C). Finally, tumor volumes were significantly smaller in fluspirilen-treated animals than in controls (Figure 7D). Immunohistochemistry performed on tissue sections from xenografts also showed that KIF20A and FOXM1 were decreased in fluspirilene-treated tumors compared to controls (Figure 7E). Taken together, the results indicated that fluspirilene suppressed GBM growth *in vitro* and *in vivo* by suppressing the FOXM1-KIF20A axis (Figure S3).

## Discussion

One of the major challenges in the treatment of GBM is that tissue drug concentrations cannot reach therapeutic levels due to the presence of the blood-brain barrier (BBB) [32, 33]. However, the inherent BBB permeability of anti-schizophrenic drugs has become a major advantage in the treatment of GBM, which occurs by multiple mechanisms. Fluvoxamine disrupts actin polymerization [34], olanzapine induces autophagy and increases temozolomide sensitivity [35, 36], and valproate inhibits classical Wnt signaling and DNA double-strand break repair [37, 38]. Fluspirilene, a potent antipsychotic, has been shown to have potent anti-GBM effects [18]. Fluspirilene has been shown to inhibit glioma stem cell proliferation and invasion by inactivating signal transducer and activator of transcription 3 (STAT3) [22]. In this study, we have shown that fluspirilene inhibits proliferation and induces apoptosis of GBM cells by suppressing the FOXM1-KIF20A axis.

KIF20A, a member of the kinesin superfamily, is a microtubule-related motor protein required for cell cycle mitosis and cell motility. KIF20A has been reported to be overexpressed in lung, gastric, bladder, renal, ovarian, and breast cancers. Previous studies have shown that KIF20A contributes to proliferation, migration, invasion, and angiogenesis in tumorigenesis [30, 31, 39–41]. In several studies, KIF20A is highly expressed in gliomas and negatively correlated with tumor prognosis [42]. KIF20A is considered a glioma neoantigen and thus a potential immunotherapeutic target. To address the issue of inter- and intra-tumoral heterogeneity of glioma cells, vaccines have been developed against several glioma neoantigens, including LY6K, DEPDC1, KIF20A, and FOXM1, as well as glioma angiogenesis-associated antigen peptides (VEGFR1 and VEGFR2). A pilot study was conducted with such vaccines in patients with recurrent high-grade glioma [43]. The treatment results verified the tolerability and immunoreactivity of these glioma-associated antigens and preliminarily demonstrated the efficacy of immunotherapy for the treatment of GBM.

Previous articles have also reported that FOXM1 regulates KIF20A at the transcriptional level in a variety of tumors [44, 45]. FOXM1 is a well-known transcription factor and a versatile protein involved in multiple biological activities, including the regulation of cell cycle G1/S and G2/M transitions, maintenance of mitotic spindle integrity, metastasis, apoptosis, angiogenesis, tissue regeneration, and DNA damage repair [46–48]. Deregulation of FOXM1 expression or any of these functions may contribute to tumorigenesis. Reprogramming of metabolism, including glucose, fatty acid, cholesterol, and amino acid metabolism, is a hallmark of cancer cells [49]. Several metabolic abnormalities have been reported to promote GBM development, progression, relapse, or treatment resistance [50]. In particular, *IDH* mutations are not only associated with a better patient prognosis but also reflect the importance of metabolic therapy in the treatment of GBM [51]. FOXM1 has been reported to be involved in aerobic glycolysis, also known as the Warburg effect in cancer cells, and to promote tumorigenesis by directly regulating the transcriptional activation of several genes involved in metabolism, such as *LDHA*, *GLUT1*, and *HK2* [50, 52]. With continued investigation, FOXM1 has the potential to emerge as an important target for cancer therapy in the future. The FOXM1-KIF20A axis in the development and progression of GBM has already attracted our attention.

Long-term clinical use of fluspirilene and similar drugs has given us more knowledge to help us make the most of their advantages and avoid their disadvantages. Although the second generation of anti-schizophrenic drugs, represented by pimozide and olanzapine, have a much lower risk of extrapyramidal side effects than the first-generation drugs, long-term use has resulted in greater metabolic side effects such as weight gain, impaired glucose metabolism [53, 54] and dyslipidemia. However, pimozide has also been shown to have anti-tumor effects [55]. Researchers also found that 13 of the top 30 upregulated genes in neuroblastoma cells (IMR32) cultured in the presence of 10 μM pimozide for 6 h are known to be involved in cholesterol biosynthesis [56]. We also found that the expression profiles of different tumor cells treated with fluspirilene showed similar changes in gene expression. We have not yet conducted experiments, but considering that cholesterol synthesis has a positive effect on GBM growth, the next step is to try to use fluspirilene in combination with synthetic anti-cholesterol drugs to treat GBM. Olanzapine (OLZ) solid lipid nanoparticles have been reported to increase bioavailability by 23-fold and prolong mean brain residence time to a greater extent than OLZ suspension alone [57]. From a pharmaceutical perspective, we can target fluspirilene to improve anti-GBM efficacy while reducing side effects.

Although long-term use of fluspirilene may have neurological and metabolic side effects, fluspirilene is a promising molecule for the treatment of GBM. However, many aspects need to be further clarified, including the mechanisms underlying its anti-tumor effects, tissue targeting, and optimization

of its molecular structure. Finally, clinical trials are needed to validate the efficacy and safety of fluspirilene in combination with temozolomide and/or radiation, which are the current standard of care for GBM. In conclusion, the present study demonstrated that fluspirilene inhibits proliferation and induces apoptosis of GBM cells by inhibiting the transcriptional activity of KIF20A. Based on these findings, further studies are warranted to investigate the precise mechanisms involved.

**Supplementary information** is available in the online version of the paper.

Acknowledgments: This work was supported by the Department of Science & Technology of Shandong Province (2017CXGC1502, 2018CXGC1503, and 2018GSF118082), the Shandong Provincial Natural Science Foundation (ZR2017MH116 and ZR2017MH015), and The Affiliated Yantai Yuhuangding Hospital of Qingdao University (YHDYY2022-12). We appreciate like to thank Professor Xingang Li, Professor Jian Wang, and Professor Bin Huang from the Neurosurgery Laboratory of Qilu Hospital of Shandong University for their selfless help in terms of experimental equipment, venues, and experimental techniques. We thank Professor Rolf Bjerkvig from the Department of Biomedicine, University of Bergen, Norway for GBM#P3 cells sincerely. We would like to thank our researchers for their hard work and reviewers for their valuable advice.

## References

[1] OSTROM QT, GITTLEMAN H, TRUITT G, BOSCIA A, KRUCHKO C et al. Cbtrus Statistical Report: Primary Brain and Other Central Nervous System Tumors Diagnosed in the United States in 2011–2015. Neuro Oncol 2018; 20(suppl_4): iv1–iv86. https://doi.org/10.1093/neuonc/noy131

[2] SHERGALIS A, BANKHEAD A, 3RD, LUESAKUL U, MUANGSIN N, NEAMATI N. Current Challenges and Opportunities in Treating Glioblastoma. Pharmacol Rev 2018; 70: 412–445. https://doi.org/10.1124/pr.117.014944

[3] GERLINGER M, ROWAN AJ, HORSWELL S, MATH M, LARKIN J et al. Intratumor heterogeneity and branched evolution revealed by multiregion sequencing. N Engl J Med 2012; 366: 883–892. https://doi.org/10.1056/NEJMoa1113205

[4] HUSE JT, HOLLAND EC. Targeting brain cancer: advances in the molecular pathology of malignant glioma and medulloblastoma. Nat Rev Cancer 2010; 10: 319–331. https://doi.org/10.1038/nrc2818

[5] WECHSLER-REYA R, SCOTT MP. The developmental biology of brain tumors. Annu Rev Neurosci 2001; 24: 385–428. https://doi.org/10.1146/annurev.neuro.24.1.385

[6] SCHAFER N, GIELEN GH, RAUSCHENBACH L, KEBIR S, TILL A et al. Longitudinal heterogeneity in glioblastoma: moving targets in recurrent versus primary tumors. J Transl Med 2019; 17: 96. https://doi.org/10.1186/s12967-019-1846-y

[7] QAZI MA, VORA P, VENUGOPAL C, SIDHU SS, MOFFAT J et al. Intratumoral heterogeneity: pathways to treatment resistance and relapse in human glioblastoma. Ann Oncol 2017; 28: 1448–1456. https://doi.org/10.1093/annonc/mdx169

[8] SHIBAO S, MINAMI N, KOIKE N, FUKUI N, YOSHIDA K et al. Metabolic heterogeneity and plasticity of glioma stem cells in a mouse glioblastoma model. Neuro Oncol 2018; 20: 343–354. https://doi.org/10.1093/neuonc/nox170

[9] HUBERT CG, RIVERA M, SPANGLER LC, WU Q, MACK SC et al. A Three-Dimensional Organoid Culture System Derived from Human Glioblastomas Recapitulates the Hypoxic Gradients and Cancer Stem Cell Heterogeneity of Tumors Found in Vivo. Cancer Res 2016; 76: 2465–2477. https://doi.org/10.1158/0008-5472.CAN-15-2402

[10] JAMPILEK J. Design and Discovery of New Antibacterial Agents: Advances, Perspectives, Challenges. Curr Med Chem 2018; 25: 4972–5006. https://doi.org/10.2174/0929867324666170918122633

[11] SILVER LL. Challenges of Antibacterial Discovery. Clin Microbiol Rev 2011; 24: 71–109. https://doi.org/10.1128/CMR.00030-10

[12] PAYNE DJ, GWYNN MN, HOLMES DJ, POMPLIANO DL. Drugs for bad bugs: confronting the challenges of antibacterial discovery. Nat Rev Drug Discov 2007; 6: 29–40. https://doi.org/10.1038/nrd2201

[13] SLEIRE L, FØRDE HE, NETLAND IA, LEISS L, SKEIE BS et al. Drug repurposing in cancer. Pharmacol Res 2017; 124: 74–91. https://doi.org/10.1016/j.phrs.2017.07.013

[14] CHA Y, EREZ T, REYNOLDS IJ, KUMAR D, ROSS J et al. Drug repurposing from the perspective of pharmaceutical companies. Br J Pharmacol 2018; 175: 168–180. https://doi.org/10.1111/bph.13798

[15] DALTON SO, JOHANSEN C, POULSEN AH, NØRGAARD M, SØRENSEN HT et al. Cancer risk among users of neuroleptic medication: a population-based cohort study. Br J Cancer 2006; 95: 934–939. https://doi.org/10.1038/sj.bjc.6603259

[16] FOND G, MACGREGOR A, ATTAL J, LARUE A, BRITTNER M et al. Antipsychotic drugs: pro-cancer or anti-cancer? A systematic review. Med Hypotheses 2012; 79: 38–42. https://doi.org/10.1016/j.mehy.2012.03.026

[17] MIYAMOTO S, DUNCAN GE, MARX CE, LIEBERMAN JA. Treatments for schizophrenia: a critical review of pharmacology and mechanisms of action of antipsychotic drugs. Mol Psychiatry 2005; 10: 79–104. https://doi.org/10.1038/sj.mp.4001556

[18] PATIL SP, PACITTI MF, GILROY KS, RUGGIERO JC, GRIFFIN JD et al. Identification of antipsychotic drug fluspirilene as a potential p53-MDM2 inhibitor: a combined computational and experimental study. J Comput Aided Mol Des 2015; 29: 155–163. https://doi.org/10.1007/s10822-014-9811-6

[19] CHEN Y, CUI Y, SUN X, WU H, OU M et al. Repurposing of antipsychotics perphenazine for the treatment of endometrial cancer. Bioorg Med Chem Lett 2020; 30: 127239. https://doi.org/10.1016/j.bmcl.2020.127239

[20] LI J, YAO QY, XUE JS, WANG LJ, YUAN Y et al. Dopamine D2 receptor antagonist sulpiride enhances dexamethasone responses in the treatment of drug-resistant and metastatic breast cancer. Acta Pharmacol Sin 2017; 38: 1282–1296. https://doi.org/10.1038/aps.2017.24

[21] SHI XN, LI H, YAO H, LIU X, LI L et al. In Silico Identification and in Vitro and in Vivo Validation of Anti-Psychotic Drug Fluspirilene as a Potential Cdk2 Inhibitor and a Candidate Anti-Cancer Drug. PLoS One 2015; 10: e0132072. https://doi.org/10.1371/journal.pone.0132072

[22] DONG Y, FURUTA T, SABIT H, KITABAYASHI T, JIAPAER S et al. Identification of antipsychotic drug fluspirilene as a potential anti-glioma stem cell drug. Oncotarget 2017; 8: 111728–11141. https://doi.org/10.18632/oncotarget.22904

[23] WANG Z, LACHMANN A, KEENAN AB, MA'AYAN A. L1000FWD: fireworks visualization of drug-induced transcriptomic signatures. Bioinformatics 2018; 34: 2150–2152. https://doi.org/10.1093/bioinformatics/bty060

[24] HUANG DW, SHERMAN BT, LEMPICKI RA. Bioinformatics enrichment tools: paths toward the comprehensive functional analysis of large gene lists. Nucleic Acids Res 2009; 37: 1–13. https://doi.org/10.1093/nar/gkn923

[25] CANCER GENOME ATLAS RESEARCH NETWORK. Comprehensive genomic characterization defines human glioblastoma genes and core pathways. Nature 2008; 455: 1061–1068. https://doi.org/10.1038/nature07385

[26] EDGAR R, DOMRACHEV M, LASH AE. Gene Expression Omnibus: NCBI gene expression and hybridization array data repository. Nucleic Acids Res 2002; 30: 207–210. https://doi.org/10.1093/nar/30.1.207

[27] THUL PJ, AKESSON L, WIKING M, MAHDESSIAN D, GELADAKI A et al. A subcellular map of the human proteome. Science 2017; 356: eaal3321. https://doi.org/10.1126/science.aal3321

[28] MADHAVAN S, ZENKLUSEN JC, KOTLIAROV Y, SAHNI H, FINE HA et al. Rembrandt: helping personalized medicine become a reality through integrative translational research. Mol Cancer Res 2009; 7: 157–167. https://doi.org/10.1158/1541-7786.MCR-08-0435

[29] KONG Y, FENG Z, CHEN A, QI Q, HAN M et al. The Natural Flavonoid Galangin Elicits Apoptosis, Pyroptosis, and Autophagy in Glioblastoma. Front Oncol 2019; 9: 942. https://doi.org/10.3389/fonc.2019.00942

[30] SHEN T, YANG L, ZHANG Z, YU J, DAI L et al. KIF20a Affects the Prognosis of Bladder Cancer by Promoting the Proliferation and Metastasis of Bladder Cancer Cells. Dis Markers 2019; 2019: 4863182. https://doi.org/10.1155/2019/4863182

[31] ZHAO X, ZHOU LL, LI X, NI J, CHEN P et al. Overexpression of KIF20A confers malignant phenotype of lung adenocarcinoma by promoting cell proliferation and inhibiting apoptosis. Cancer Med 2018; 7: 4678–4689. https://doi.org/10.1002/cam4.1710

[32] YANG JP, YANG JK, LI C, CUI ZQ, LIU HJ et al. Downregulation of ZMYND11 induced by miR-196a-5p promotes the progression and growth of GBM. Biochem Biophys Res Commun 2017; 494: 674–680. https://doi.org/10.1016/j.bbrc.2017.10.098

[33] SCHNEIDER SW, LUDWIG T, TATENHORST L, BRAUNE S, OBERLEITHNER H et al. Glioblastoma cells release factors that disrupt blood-brain barrier features. Acta Neuropathol 2004; 107: 272–276. https://doi.org/10.1007/s00401-003-0810-2

[34] HAYASHI K, MICHIUE H, YAMADA H, TAKATA K, NAKAYAMA H et al. Fluvoxamine, an anti-depressant, inhibits human glioblastoma invasion by disrupting actin polymerization. Sci Rep 2016; 6: 23372. https://doi.org/10.1038/srep23372

[35] ZHU Y, ZHAO YF, LIU RS, XIONG YJ, SHEN X et al. Olanzapine induced autophagy through suppression of NF-κB activation in human glioma cells. CNS Neurosci Ther 2019; 25: 911–921. https://doi.org/10.1111/cns.13127

[36] KARPEL-MASSLER G, KAST RE, WESTHOFF MA, DWUCET A, WELSCHER N et al. Olanzapine inhibits proliferation, migration and anchorage-independent growth in human glioblastoma cell lines and enhances temozolomide's antiproliferative effect. J Neurooncol 2015; 122: 21–33. https://doi.org/10.1007/s11060-014-1688-7

[37] RIVA G, CILIBRASI C, BAZZONI R, CADAMURO M, NEGRONI C et al. Valproic Acid Inhibits Proliferation and Reduces Invasiveness in Glioma Stem Cells through Wnt/β Catenin Signalling Activation. Genes 2018; 9: 522. https://doi.org/10.3390/genes9110522

[38] PATTIES I, KORTMANN RD, GLASOW A. Inhibitory effects of epigenetic modulators and differentiation inducers on human medulloblastoma cell lines. J Exp Clin Cancer Res 2013; 32: 27. https://doi.org/10.1186/1756-9966-32-27

[39] YAN GR, ZOU FY, DANG BL, ZHANG Y, YU G et al. Genistein-induced mitotic arrest of gastric cancer cells by downregulating KIF20A, a proteomics study. Proteomics 2012; 12: 2391–2399. https://doi.org/10.1002/pmic.201100652

[40] XIU G, SUI X, WANG Y, ZHANG Z. FOXM1 regulates radiosensitivity of lung cancer cell partly by upregulating KIF20A. Eur J Pharmacol 2018; 833: 79–85. https://doi.org/10.1016/j.ejphar.2018.04.021

[41] KAWAI Y, SHIBATA K, SAKATA J, SUZUKI S, UTSUMI F et al. KIF20A expression as a prognostic indicator and its possible involvement in the proliferation of ovarian clear-cell carcinoma cells. Oncol Rep 2018; 40: 195–205. https://doi.org/10.3892/or.2018.6401

[42] SAITO K, OHTA S, KAWAKAMI Y, YOSHIDA K, TODA M. Functional analysis of KIF20A, a potential immunotherapeutic target for glioma. J Neurooncol 2017; 132: 63–74. https://doi.org/10.1007/s11060-016-2360-1

[43] KIKUCHI R, UEDA R, SAITO K, SHIBAO S, NAGASHIMA H et al. A Pilot Study of Vaccine Therapy with Multiple Glioma Oncoantigen/Glioma Angiogenesis-Associated Antigen Peptides for Patients with Recurrent/Progressive High-Grade Glioma. J Clin Med 2019; 8: 263. https://doi.org/10.3390/jcm8020263

[44] NESTAL DE MORAES G, DELBUE D, SILVA KL, ROBAINA MC, KHONGKOW P et al. FOXM1 targets XIAP and Survivin to modulate breast cancer survival and chemoresistance. Cell Signal 2015; 27: 2496–2505. https://doi.org/10.1016/j.cellsig.2015.09.013

[45] CHEN Y, LIU Y, NI H, DING C, ZHANG X et al. FoxM1 overexpression promotes cell proliferation and migration and inhibits apoptosis in hypopharyngeal squamous cell carcinoma resulting in poor clinical prognosis. Int J Oncol 2017; 51: 1045–1054. https://doi.org/10.3892/ijo.2017.4094

[46] LIN SC, KAO CY, LEE HJ, CREIGHTON CJ, ITTMANN MM et al. Dysregulation of miRNAs-COUP-TFII-FOXM1-CENPF axis contributes to the metastasis of prostate cancer. Nat Commun 2016; 7: 11418. https://doi.org/10.1038/ncomms11418

[47] WANG Y, YUN Y, WU B, WEN L, WEN M et al. FOXM1 promotes reprogramming of glucose metabolism in epithelial ovarian cancer cells via activation of GLUT1 and HK2 transcription. Oncotarget 2016; 7: 47985–47997. https://doi.org/10.18632/oncotarget.10103

[48] YOSHIDA Y, WANG IC, YODER HM, DAVIDSON NO, COSTA RH. The forkhead box M1 transcription factor contributes to the development and growth of mouse colorectal cancer. Gastroenterology 2007; 132: 1420–1431. https://doi.org/10.1053/j.gastro.2007.01.036

[49] VANDER HEIDEN MG. Targeting cancer metabolism: a therapeutic window opens. Nat Rev Drug Discov 2011; 10: 671–684. https://doi.org/10.1038/nrd3504

[50] DUMAN C, YAQUBI K, HOFFMANN A, ACIKGOZ AA, KORSHUNOV A et al. Acyl-Coa-Binding Protein Drives Glioblastoma Tumorigenesis by Sustaining Fatty Acid Oxidation. Cell Metab 2019; 30: 274–289. https://doi.org/10.1016/j.cmet.2019.04.004

[51] DANG L, JIN S, SU SM. IDH mutations in glioma and acute myeloid leukemia. Trends Mol Med 2010; 16: 387–397. https://doi.org/10.1016/j.molmed.2010.07.002

[52] CUI J, SHI M, XIE D, WEI D, JIA Z et al. FOXM1 promotes the warburg effect and pancreatic cancer progression via transactivation of LDHA expression. Clin Cancer Res 2014; 20: 2595–2606. https://doi.org/10.1158/1078-0432.CCR-13-2407

[53] CHEN CH, SHYUE SK, HSU CP, LEE TS. Atypical Antipsychotic Drug Olanzapine Deregulates Hepatic Lipid Metabolism and Aortic Inflammation and Aggravates Atherosclerosis. Cell Physiol Biochem 2018; 50: 1216–1229. https://doi.org/10.1159/000494573

[54] STAPEL B, KOTSIARI A, SCHERR M, HILFIKER-KLEINER D, BLEICH S et al. Olanzapine and aripiprazole differentially affect glucose uptake and energy metabolism in human mononuclear blood cells. J Psychiatr Res 2017; 88: 18–27. https://doi.org/10.1016/j.jpsychires.2016.12.012

[55] DAKIR EH, PICKARD A, SRIVASTAVA K, MCCRUDDEN CM, GROSS SR et al. The anti-psychotic drug pimozide is a novel chemotherapeutic for breast cancer. Oncotarget 2018; 9: 34889–34910. https://doi.org/10.18632/oncotarget.26175

[56] WIKLUND ED, CATTS VS, CATTS SV, NG TF, WHITAKER NJ et al. Cytotoxic effects of antipsychotic drugs implicate cholesterol homeostasis as a novel chemotherapeutic target. Int J Cancer 201; 126: 28–40. https://doi.org/10.1002/ijc.24813

[57] NATARAJAN J, BASKARAN M, HUMTSOE LC, VADIVELAN R, JUSTIN A. Enhanced brain targeting efficacy of Olanzapine through solid lipid nanoparticles. Artif Cells Nanomed Biotechnol 2017; 45: 364–371. https://doi.org/10.3109/21691401.2016.1160402

https://doi.org/10.4149/neo_2024_230909N479

# Fluspirilene exerts an anti-glioblastoma effect through suppression of the FOXM1-KIF20A axis

Yang KONG[1,2], Wei ZHU[2], Zhen ZHANG[2,3], Wei SUN[2], Guangqiang CUI[2], Hongguang CHEN[2], Haiying WANG[4,*]

## Supplementary Information

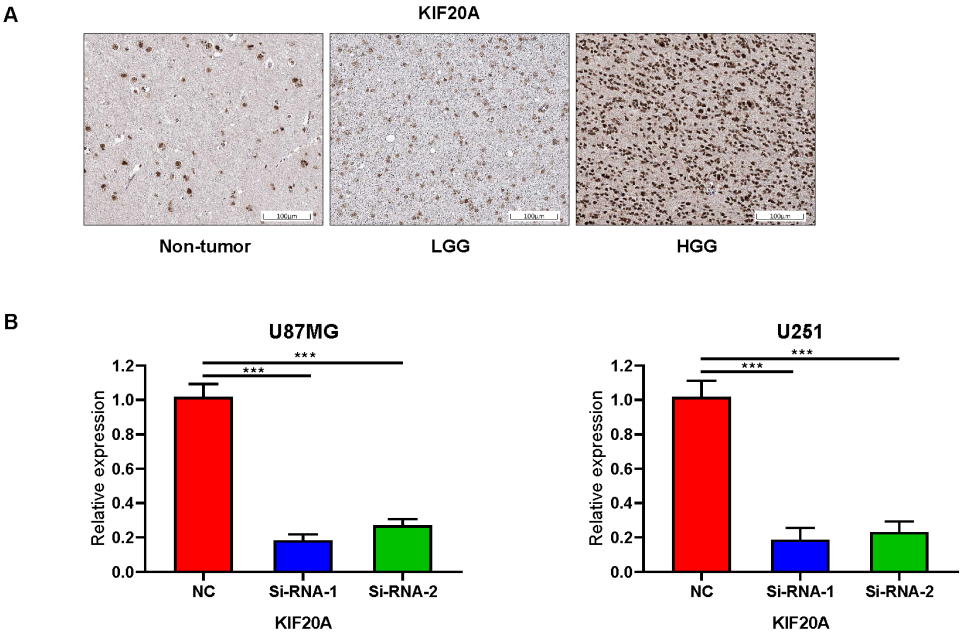


**Figure S1. A) Images of immunohistochemical staining for KIF20A in non-neoplastic brain tumor tissue, low-grade glioma, and GBM (scale bars: 100 μm; derived from HPA database). B) Graphic representation of qRT-PCR to validate the efficiency of si-KIF20A in U87MG and U251 cells. GAPDH was used as an internal reference .***p<0.001 compared to the control.**

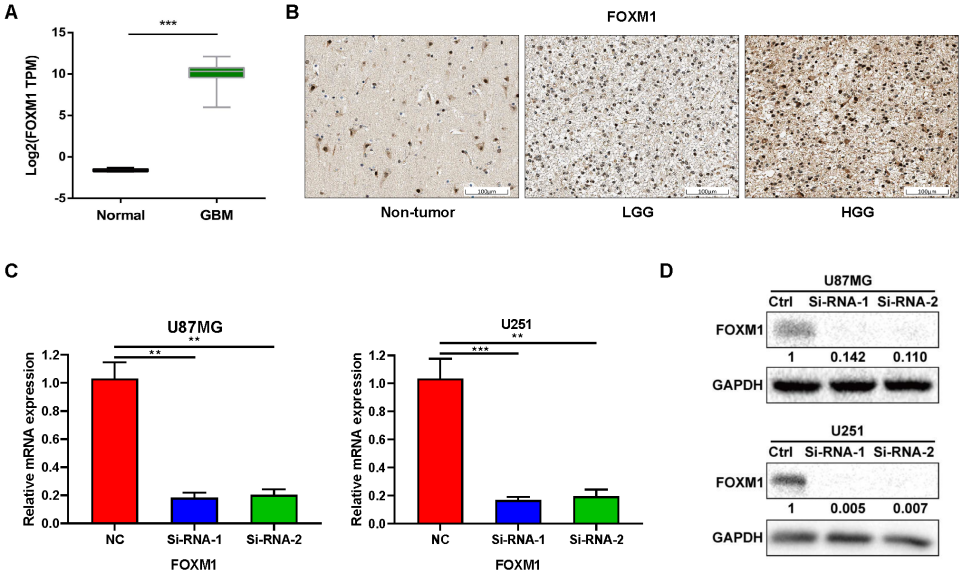


**Figure S2. A) Graphic representation of the mRNA expression of *FOXM1* in non-neoplastic brain tissue and GBM in TCGA database. B) Images of immunohistochemical staining for FOXM1 in non-neoplastic brain tissue, low-grade glioma, and GBM (scale bars: 100 μm; derived from HPA database). C) Fluorescence images of EdU incorporation and statistical results from U87MG and U251 cells after siRNA knockdown of FOXM1. D) Western blot to validate the efficiency of si-FOXM1 in U87MG and U251 cell lines. GAPDH was used in the protein loading control. *p<0.01; ***p<0.001 compared to the control.**

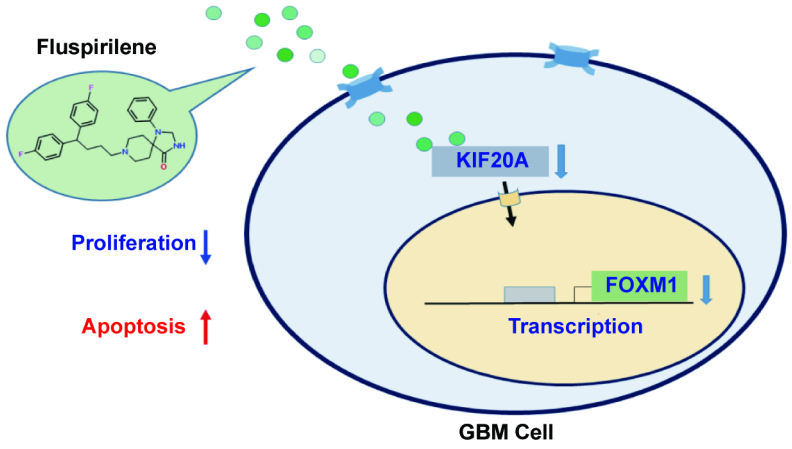


**Figure S3. Hypothetical model for the anti-GBM mechanism of fluspirilene. Briefly, fluspirilene downregulates the protein levels of FOXM1, thus reducing transcription of KIF20A, and leading to increased apoptosis and inhibition of proliferation of GBM cells.**